Chemosphere 307 (2022) 135638

Contents lists available at ScienceDirect

Chemosphere

journal homepage: www.elsevier.com/locate/chemosphere

Evaluation of biostimulation, bioaugmentation, and organic amendments application on the bioremediation of recalcitrant hydrocarbons of soil

Sandra Curiel-Alegre [a,b], Blanca Velasco-Arroyo [a], Carlos Rumbo [a], Aqib Hassan Ali Khan [a], Juan Antonio Tamayo-Ramos [a], Carlos Rad [a], José Luis R. Gallego [c], Rocío Barros [a,*]

[a] International Research Center in Critical Raw Materials for Advanced Industrial Technologies (ICCRAM), University of Burgos, Centro de I+D+I. Plaza Misael Bañuelos s/n. 09001, Burgos, Spain
[b] Research Group in Composting (UBUCOMP), University of Burgos, Faculty of Sciences, Plaza Misael Bañuelos s/n, 09001, Burgos, Spain
[c] Environmental Biogeochemistry & Raw Materials Group and INDUROT, Campus de Mieres, University of Oviedo, C/ Gonzalo Gutiérrez Quirós s/n, 33600, Mieres, Spain

HIGHLIGHTS

- Bioaugmentation with vermicompost improves hydrocarbon degradation by up to 34.4%.
- Bioremediation effectively removes the non-recalcitrant hydrocarbons in soil.
- Biodegradable compounds, like aromatics and branched alkanes, are less depleted.
- High molecular weight hydrocarbons are recalcitrant to soil microbial activity.

GRAPHICAL ABSTRACT

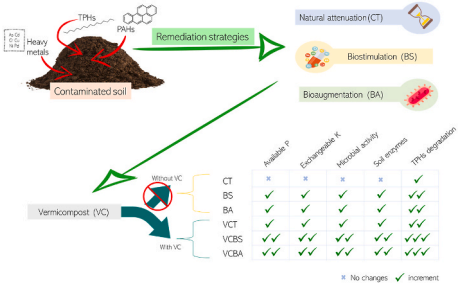

ARTICLE INFO

Handling Editor: X. Cao

Keywords:
Biostimulation
Bioaugmentation
Phospholipid fatty acids
Total petroleum hydrocarbons polluted soils
Soil enzymes

ABSTRACT

In the present work, the operational conditions for improving the degradation rates of Total Petroleum Hydrocarbons (TPHs) in contaminated soil from a machinery park were optimized at a microcosms scale along a 90-days incubation period. In this study, bioremediation strategies and an organic amendment have been tested to verify the remediation of soil contaminated with different hydrocarbons, mineral oils, and heavy metals. Specifically, designed biostimulation and bioaugmentation strategies were compared with and without adding vermicompost. The polluted soil harboring multiple contaminants, partially attenuated for years, was used. The initial profile showed enrichment in heavy linear alkanes, suggesting a previous moderate weathering. The application of vermicompost increased five and two times the amounts of available phosphorus (P) and exchangeable potassium (K), respectively, as a direct consequence of the organic amendment addition. The microbial activity increased due to soil acidification, which influenced the solubility of P and other micronutrients. It also impacted the predominance and variability of the different microbial groups and the incubation, as reflected by phospholipid fatty acid (PLFA) results. An increase in the alkaline phosphatases and proteases linked to bacterial growth was displayed. This stimulation of microbial metabolism correlated with the degradation rates since TPHs degradation' efficiency after vermicompost addition reached 32.5% and 34.4% of the initial hydrocarbon levels for biostimulation and bioaugmentation, respectively. Although Polycyclic Aromatic

* Corresponding author.
E-mail address: rbarros@ubu.es (R. Barros).

https://doi.org/10.1016/j.chemosphere.2022.135638
Received 6 May 2022; Received in revised form 1 July 2022; Accepted 4 July 2022
Available online 8 July 2022

Hydrocarbons (PAHs) were less abundant in this soil, results also decreased, especially for the most abundant, the phenanthrene. Despite improving the degradation rates, results revealed that recalcitrant and hydrophobic petroleum compounds remained unchanged, indicating that mobility, linked to bioavailability, probably represents the limiting step for further soil recovery.

1. Introduction

Modern economies are characterized by a strong dependence on fossil fuels (Sima et al., 2019). However, increasing the frequency of accidental oil spills and the release of petroleum derivatives cause significant environmental impacts and pose substantial hazards to human health (Hussain et al., 2022; Khan et al., 2019). Despite numerous studies focused on decontamination strategies, it remains crucial to gain new, innovative, and sustainable techniques to reduce, degrade, and remove diverse pollutants in soils, sediments, and water bodies. Conventional technologies for cleaning-up contaminated soils (excavation, landfilling, and soil washing) and waters (treatment with activated carbon or ion exchange resins) are generally energy-intensive, expensive, time-consuming, and waste-producing (Yousaf et al., 2022). These technologies are not efficient for treating moderate to low-level polluted sites, which still pose human health and environmental risk. Bioremediation for oil-contaminated soils and sediments is a cost-effective and sustainable clean-up technology (Hussain et al., 2018). These include landfarming, bio-piling, phytoremediation, biostimulation and bioaugmentation (Mair et al., 2013). Biostimulation (BS) and bioaugmentation (BA) have unveiled good results based on improving hydrocarbons biodegradation. The difference between these two methods is that, in the case of bioaugmentation, the basis is the inoculation of exogenous degrading microorganisms into the soil (Wu et al., 2017). At the same time, biostimulation consists of the promotion of the degradation capacity of the autochthonous microbial communities by the addition of nutrients' optimized formulas, carrier materials, and amendments to stimulate the metabolic functions of the microorganisms that can use the contaminants present in the soils as "feeding" sources (Khan et al., 2017).

Applying soil amendments with organic residues raises the soil's organic matter (OM), a crucial property intimately linked to soil fertility (Iqbal et al., 2020). The OM helps stimulate microbial activities, mineralize resistant materials, and eliminate xenobiotic compounds by promoting biotic and abiotic processes that rely on biodegradation and adsorption mechanisms (Mushtaq et al., 2020). Composting polluted soils and organic wastes or adding compost to the soil is a commonly used soil bioremediation economic method (Chen et al., 2015). The aerobic bio-decomposition of organic waste reduces biowaste volume by 40–50% and provides a product that acts as a soil conditioner or biofertilizer along with polluted soil remediation (Iqbal et al., 2020; Wu et al., 2017). Vermicomposts (product of the decomposition process using various species of worms) have significantly larger nutrients than composts and result in higher microbial population size and activity (Das and Deka, 2021). The hydrocarbon remediation process is highly dependent on the pollutant load. An increased pollutant load can delay the profits of remediation using microorganisms (Hussain et al., 2022). Apart from this, the hydrocarbon-impacted soil remediation process is highly dependent on aeration, nutrients content, organic matter, CN ratio and the presence of the hydrocarbon-degrading microbial population (Yousaf et al., 2022). Even if all these factors are maintained to optimal, the biggest challenge to treatment is associated with aged or weathered hydrocarbon-contaminated soils. The aging of hydrocarbon in the soil makes the treatment process much more complex, leading to the heterogeneous spatial distribution of the pollutants, soil structure deterioration, nutrient imbalance, and hydrophobicity. The increased hydrophobicity leads to high sorption of recalcitrant PAHs fractions between soil pores. It causes soil aging, makes the hydrocarbon less bio-accessible, and reduces the soil moisture and water retention capacity (Hussain et al., 2018).

Despite all these known issues, much of the focus in the previously published research work has remained on the spiked contaminated soils that lack the aging hydrocarbon effect, while the aged hydrocarbon contaminated soil has always remained a grey area in research and requires due attention. Hence the objective of the current study has been to encounter new bioremediation solutions to optimize the treatment of soils contaminated with total petroleum hydrocarbons (TPHs), including polycyclic aromatic hydrocarbons (PAHs), in the presence of potentially toxic metals and metalloids. Accordingly, specifically designed biostimulation and bioaugmentation strategies have been tested and compared to quantify the efficacy of the hydrocarbon remediation strategy. The targeted soil matrix has been challenging since it harbors a contamination history showing around recalcitrant long-chain hydrocarbons (C21-30), exhibiting a low bioavailability after a long natural attenuation lasting for years.

2. Materials and methods

2.1. Chemicals and reagents

For chromatographic separation quality aliphatic hydrocarbons: Alkanes-Mix 12, 100 μg mL^{-1} in toluene (C_7H_8), C8–C40 (pair no. of C, 17 HC) and polyaromatic hydrocarbons: PAHs-Mix 9, in cyclohexane (100 μg mL^{-1}) were supplied by LGC standards (details in supplementary material). The certified reference CRM-357 and CRM-359 for TPH–sandy loam and TPH–clay was used, respectively (Sigma-Aldrich). Isolute Sorbent EPH (25 mL 5 g^{-1}) extraction cartridges for sample extraction and elution were used (Biotage) in the SPE-24G column processor (JT Baker). Extraction solvents, GC grade acetone (C_3H_6O), dichloromethane (DCM), internal standard nonadecanoic acid (C19:0), and hexane (hx), and reagents for phospholipid fatty acids (PLFAs) determination, the analytical grade for chromatography; bacterial acid methyl ester (BAME) mix and Supelco 37 component fatty acid methyl esters (FAME) mix (CRM47885), were provided by Sigma Aldrich.

2.2. Nutrient solutions and inoculum preparation

Modified BHB (Bushnell Haas Broth) solutions were prepared, either for biostimulation or bioaugmentation (BHB-2) or for the treatments with VC (BHB-3), in which the amount of N supplemented by the VC was subtracted from the nutrient solution, considering a mineralization coefficient of 30% (Khan et al., 2016a). BHB-2 was prepared by mixing individual solutions to reach the following added amounts (g kg^{-1} dry soil): $CaCl_2$ 0.0061; KH_2PO_4 0.3058; K_2HPO_4 0.3058; $MgSO_4$ 0.0612; NH_4NO_3 3.5425; $FeCl_3$ 0.0153. the $FeCl_3$ was added separately to avoid precipitation. BHB-3 had the same saline composition, except NH_4NO_3 3.0454 (g kg^{-1} dry soil basis).

The consortium used as inoculant was isolated from the same soil used in this study by serial enrichment cultures, using diesel (10 g/L) as the sole carbon and energy source (Garrido-Sanz et al., 2019). The consortium harbors around 50 OTUs and is composed by *Enterobacteriaceae* (33,56%), followed by *Pseudomonadaceae* (26,61%) *Burkholderiaceae* (24,35%), *Moraxellaceae* (3,64%), *Xantomonadaceae* (4,40%), *Rhizobiaceae* (2,42%), *Sphingomonadaceae* (1,87%) and *Rhodanobacteriaceae* (1,00%). All other families are below 1%. An aliquot of this consortium from glycerol stock was inoculated in a 20 mL minimal medium with gas oil (1% v:v) as a carbon source and incubated in a rotary shaker at 150 rpm at 28 °C overnight. After this incubation, the

culture was centrifuged and resuspended in 20 mL of minimal medium. To prepare the pre-inoculum, 2 mL of this culture were inoculated in 200 mL of minimal medium with gas oil and cultured for 2 days in the mentioned conditions. This pre-inoculum was used to inoculate six Erlenmeyer flasks containing 2 L of minimal medium with gas oil, which was incubated for 4 days in the same conditions (20 mL of pre-inoculum per flask). Cultures were then centrifuged at 3,800 *g* and 8 °C for 30 min. Supernatants were discarded, and pellets were resuspended in a minimal medium, divided into 2 equal halves, and centrifuged again to remove the remnants of the culture medium with gasoil used for consortium growth. Finally, one of the obtained pellets was resuspended in 200 mL of BHB-2, while the other was resuspended into 200 mL of BHB-3. Both samples were transferred to a 250 mL volumetric flask. Aliquots of these suspensions were collected for CFU (Colony Forming Unit) counting and inoculum preparation.

2.3. Soil properties and characterization

The soil under study corresponds to a machinery park area in Noblejas (Toledo, Spain),contaminated with different hydrocarbons, mineral oils, and heavy metals. Air-dried soil samples were sieved at 2 mm and characterized in their physicochemical properties according to standard methods. Soil pH (H_2O, 1:5, w:v) was determined using 5 g of soil sample and 25 mL deionized water after 30 of agitation at 60 RPMs using a pH meter (GLP21, Crison). After pH determination, the soil suspension was centrifuged for 20 min at 2,000 *g*, filtered, and the electrical conductivity (EC) was measured using a conductivity meter (GLP31, Crison).

Soil available P was assessed with the help of the Olsen method. Briefly, 2 g of dry soil was extracted with 40 mL 0.5 M $NaCO_3$ at pH 8.5 after shaking for 30 min at 60 RPMs. After centrifugation, the extract was analyzed and quantified using the molybdenum blue method for orthophosphate on an autoanalyzer (San++, Skalar). Available macronutrients and trace elements were analyzed using Mehlich 3 method (Mehlich, 1984). Briefly, 20 mL of extraction solution (0.2 M CH_3COOH, 0.001 M EDTA, 0.013 M HNO_3, 0.015 M NH_4F, and 0.25 M NH_4NO_3) were mixed with 2 g dry soil (1:10, w:v), agitated for 5 min at 120 RPMs, centrifuged at 2,000 *g* for 10 min and filtered (Whatman No. 42). Nutrients and trace elements were determined in the extracts using an ICP-OES (Genesis, Spectro).

Soil organic carbon and nitrogen were measured using 0.5 M K_2SO_4 (1:8, w:v) as extractant. These extracts were centrifuged at 60 RPMs for 45 min and filtered. Then the extracts were subjected to organic C and total N analysis via a TOC-V CSN autoanalyzer (Shimadzu). Soluble ammonium and nitrate were also determined in these extracts on an autoanalyzer using the indophenol blue method and Griess reaction after reducing nitrate in a copperized-cd column, respectively (San++ Skalar, Breda).

Basal soil respiration (BSR) was articulated as mg CO_2–C kg^{-1} dry soil h^{-1}. For this activity, frozen soil samples (20 g) were attemperated for 72 h at 22 ± 0.5 °C and placed in 1-Liter jars with hermetic sealing caps. The jar was provided with a beaker, acting as a gas trap, containing 4 mL of 0.5 M NaOH. After 24 h of incubation, 2 mL of 0.5 M $BaCl_2$ were added, which led to the barium carbonate-adsorbed CO_2 precipitation. Using 0.1 M HCl through an automatic titrator (718 Stat Titrino, Metrohm), the remaining NaOH was quantified.

2.4. Experimental setup and microcosms preparation

The study was conducted at a laboratory scale in microcosms conditions for 90 days. Six treatments have been tested, including natural attenuation as a control, biostimulation with an improved nutrient formula, biostimulation with vermicompost (VC), and the same treatments with bioaugmentation. In the case of the bioaugmentation treatments, the microbial consortia inoculated corresponded to the native microbial population previously isolated from the soil site under research, which has been characterized and cultured as part of the tasks developed within the framework of the European GREENER project. In the presence and absence of VC, six different incubation treatments were prepared using biostimulation and bioaugmentation strategies. These included control soil (abbreviated as CT), biostimulation of soil (added with BHB-2, abbreviated as BS), bioaugmentation of soil (inoculated with consortium suspended in BHB-2, abbreviated as BA), vermicompost amended control soil (abbreviated as VCT), VC aided BS of soil (VC + BHB-3, abbreviated as VCBS), and VC aided BA of soil (VC + consortium suspended in BHB-3, abbreviated as VCBA). The CT was a control of natural attenuation effects over the bioremediation soil. Prior to the initiation of the experiments, the polluted soil was sieved to 2 mm and watered to reach 40% of soil water holding capacity (SWHC); to highlight, on day 43rd, when the second consortia inoculation was carried out, the SWHC was increased to 50%, using this volume of water to introduce the inoculum and nutrient solutions. Each treatment was prepared by mixing soil, amendments, and solutions using a concrete mixer and immediately distributed by weighing 200 g of dried soil into 1 L hermetic containers. A final concentration of 10^{11} CFU kg^{-1} soil was applied for the respective BA treatments. The same procedure was repeated for the second inoculation (on the 43rd day), but the final suspension was made in 100 mL of nutrient solutions. Samplings were taken 2, 15, 30, 45, 60, and 90 days of treatment. Four experimental replicates for each sampling point and treatment were maintained. The incubation was conducted in a chamber under controlled temperature conditions (22 ± 0.5 °C). Individual microcosms were opened and mixed weekly (twice) to control the moisture and soil aeration. At the end of each sampling point, soil samples were divided to perform different types of analysis: 70 g was dried in an oven at 30 °C for 48 h, and the remaining fraction was frozen at −20 °C for subsequent experiments. Control samples of day 0 for each treatment were also included.

2.5. EPH quantification, LC fractionation and GC-MS qualitative study

Extractable petroleum hydrocarbons (EPH) were extracted from 1 g soil samples (dried at 30 °C) and 20 mL of mixture C_3H_6O: hx (hexane) (1:1, v:v) in a microwave extraction oven (Ethos X, Milestone, Sorisole, Italy) at 150 °C for 20 min. The cold mixture was subjected to centrifugation for 30 min at 2,500 *g*. The resulting supernatant was filtered (though 0.22 μm filter) and evaporated to a volume of 1 mL in a rotary evaporator (SAVANT SPD111V, Thermo). Before sample loading, the extraction cartridges were conditioned with 30 mL hx, preventing the drying of cartridges. After loading the sample at ambient pressure, elution was performed using 12 and 20 mL of hx and DCM (dichloromethane). The two fractions produced were evaporated above 1 mL and injected into a Varian 3900 gas chromatography (GC) instrument provided with a flame ionization detector (FID) device and a Varian CP8907 capillary column (25 m, 0.25 mm inner diameter, with the film thickness of 0.25 mm). Spitless injection mode was performed with 250 °C of injection temperature and 3 μL of injection volume. The oven operating conditions were: initial temperature 80 °C, raising to 200 °C at 7 °C min^{-1}, then reaching 300 °C at 11 °C min^{-1}, which was maintained for 17 min. Helium was the carrier gas (74 kPa). The FID operated at 325 °C and 20 Hz. The detected aliphatic and aromatic fractions were defined based on carbon or equivalent ranges. Equivalent carbon numbers denote an assigned value to a petroleum mixture fraction, empirically derived from the fraction normalized boiling point compared to the boiling point of n-alkanes or the n-alkanes retention time in a boiling point GC column. Hydrocarbon extraction was performed with 90-day samples for all tested treatments.

An additional fingerprint study was carried out for some samples using GC-MS after LC (Liquid Chromatography) fractionation. In a Soxtherm system, using 3:1 DCM to methanol (MeOH), the soil samples (5 g) were extracted (Gerhardt analytical systems). Rotary evaporation was performed to concentrate the extracts. Extract aliquots were subjected to fractionation and gravimetrically quantified using open

column LC. Using hx and DCM as eluents, maltenes and asphaltenes were segregated using 0.45 μm filters. Maltenes were further fractionated into three fractions using LC columns, filled with silica gel and alumina. Aliphatic hydrocarbons (Fraction 1) through hx, aromatic hydrocarbons (fraction 2) with DCM: hx (7:3, v:v), while polar compounds (fraction 3) using DCM: MeOH (1:1, v:v), were eluted.

LC fractions were analyzed with GC-MS (QP-2010 Plus, Shimadzu). Helium as carrier gas at 1 mL min^{-1} was used in the capillary column (DB-5 ms). The specification of the capillary column was 60 m × 0.25 mm i.d. × 0.25 μm film (Agilent Technologies), packed with phenyl and dimethylpolysiloxane at 5:95%, respectively. The initial temperature of the oven was maintained at 50 °C for 2 min. Later the temperature was ramped at 2.5 °C min^{-1} up to 310 °C and maintained for 45 min. The GC-MS worked in electron ionization (EI) mode at 70 eV, with autotuning calibrations performed using perfluorotributylamine. The full-scan mode was used to obtain the chromatograms, with mass range for acquisition ranging from 45 to 500 m z^{-1}. NIST 2014 Mass Spectral Library (NIST 2014/EPA/NIH) was used to identify the compounds.

2.6. Soil enzyme activities

Enzyme activities were measured using fluorogenic MUF or AMC-substrates in 96-microtiter plates (Marx et al., 2001). The studied activities included acid phosphatases (EC 3.1.3.2 – AcPA), alkaline phosphatase (EC 3.1.3.3 – AlkPA), α-glucosidases (EC 3.2.1.20 – aGA), β-glucosidases (EC 3.2.1.21 – bGA), N-acetyl-β-glucosaminidase (EC 3.2.1.30 - bNAG), β-xylosidase (EC 3.2.2.27 - bXyl), leucine-aminopeptidase (EC 3.4.11.1 - LeuAMP) and sulfatase (EC 3.1.6.1 - AS). These activities were analyzed using amino-4-methylcoumarin (AMC) and 4-methylumbelliferone (MUF) derivatives as substrates. A frozen sample (1 g oven-dry) was suspended in 20 mL of deionized water in sterilized conditions. For homogenous suspension, soil samples (ice cold) were subjected to pulsed sonication (40 W) for 2 min. Aliquots of 50 μL were used for analysis with eight analytical replicates. 50 μL Modified universal buffer (MUB) at 500 μM was used to analyze each enzymatic activity. Specifically, MUB for AcPH and bGA has a pH of 5, for the activities of aGA, AS, bNAG, and bXyl pH was maintained at 6, while pH 9 and 10 were kept for AlkPA and LeuAMP, respectively. Plates were sealed to prevent evaporation and kept at 30 °C for 180 min under agitation at 150 RPMs. Tris buffer (50 μL) at pH 12 was added to stop the reaction and immediately analyzed using a fluorometric plate-reader (GENios, TECAN) with 360 and 450 nm excitation and emission filters. Fluorescence was converted into an amount of MUB or AMC according to calibration standards (0–1,500 pmol) prepared on each plate to consider the degree of fluorescence quenching through soil particles and OM.

2.7. Determination of phospholipid fatty acids

Bligh and Dyer (1959) proposed method to extract the PLFAs, was used. Chloroform ($CHCl_3$) was used to redissolution lipid fractions, and the fractions were later added to silica columns. Fractions of neutral lipid and glycolipid were eliminated using $CHCl_3$ and C_3H_6O (respectively), and phospholipids were eluted using MeOH and dried with the help of rotary evaporation. The sample was redissolved with C_7H_8 and added with an internal standard (C19:0, Sigma-Aldrich). Alkaline methanolysis was performed to make fatty acid methyl esters (FAMEs) derivates. The FAMEs were extracted using 2 mL hx twice, followed by drying and redissolution n-octane (100 μL). Agilent 6890 N GC system was used for FAMEs quantification. The system provided FID detection with a Supelco Omegawax 320 fused silica column (30 m in length), film 0.25 μm, ID 0.32. The operation temperature program of the system was as follows 140–170 °C at 2 °C min^{-1}, maintained for 30 min, followed by 170–260 °C at 5 °C min^{-1}, maintained for 20 min. Commercial standards, BacMix and FAMEmix (Sigma Aldrich), were used for the FAME peaks identification, as proposed by Palojärvi (2006).

The individual FAMEs abundance was expressed in nmol g^{-1} of dry soil. Fatty acids i15:0, a15:0, i16:0, 10 Me16:0, i17:0, Me18:0 (PLFA Gram+) were used for the representation of Gram-positive bacteria, while c16:1w9c, cy17:0, and cy19:0 (PLFA Gram-) for Gram-negative bacteria. The sum of both represents total bacterial PLFAs (PLFA Bacteria). Fungal PLFA was considered the sum of c18:2ω6,9t and c18:2ω6,9c (PLFA Fungi), and the sum of 10Me16:0 and 10Me18:0 was considered for Actinobacteria. The sum of all fatty acids quantified total PLFA to represent total microbial biomass.

2.8. Statistical analysis

The mean and the standard error of at least three independent experimental replicates were calculated for all variables. Normality and homogeneity of variances assumptions were assessed with Kolmogorov-Smirnov and Levene tests, respectively, using treatment as the fixed factor, and the data were analyzed with ANOVA (ANalysis Of VAriance) with a significance of $p \leq 0.05$. Then, the treatments were compared with the Tukey's or Dunnett's (only for PAHs) posthoc tests. All statistical analysis was performed on a statistical package for social sciences (v22.0 for Windows).

3. Results

3.1. Soil and organic amendment characterization

Soil collected from the machinery park area in Noblejas was sandy-loam texture (11.8 clay, 29.8 silt, and 58.3 sand, percent respectively), with bulk density 1.51 g cm^{-3}, highest water retention capacity (HWRC) 25.33%, pH (1:5) 7.1, electrical conductivity (EC 1:5) 0.839 dS m^{-1}, loss on ignition (LOI) 3.85%, oxidizable organic carbon 2.59%, total N 0.02%, nutrients (mg kg^{-1}): NH_4–N 2.99; NO_3–N 0.14; PO_4–P 0.10, lime content 35.08%, trace elements (mg kg^{-1}): As 77.3; Cd 7.8; Cr 14.9; Cu 8.5; Ni 9.9; Pb 339.2; Zn 680.5, and total petroleum hydrocarbons (TPHs): 4051.0 mg kg^{-1}.

As an organic amendment, vermicompost (VC) from agro-industrial wastes (ROPULPAT, Spain) was used at a rate of 2% (w:w). Physicochemical VC properties were as follows: pH (1:5) 7.0, EC (1:5) 3.157 dS m^{-1}, total organic carbon (TOC) 33.3%, and total nitrogen (TN) 2.9%. VC has been included as an organic amendment since it, in principle, leads to better hydrocarbons' adsorption, filtering, and degradation.

3.2. Biodegradation of TPHs

To understand and compare the potential degradation efficiency of the treatments under study, the quantity of extractable petroleum hydrocarbons (EPHs) and their correspondent aliphatic and aromatic fractions (see below for details) was analyzed after 90 days of microcosms incubation. The EPHs content was reduced from the initial 4051.0 mg kg^{-1} dry soil to 3806.0 mg kg^{-1} in the case of the control soil (CT), to 3,098.5 mg kg^{-1} in the case of the biostimulation treatment (BS), and 2864.5 mg kg^{-1} after applying the microbial consortium (BA), which represents a reduction of 6.0%, 23.5% and 29.3% of the initial content, respectively (Fig. 1A). Likewise, EPHs were reduced by applying 2% (w w^{-1}) vermicompost (VCT) to 3640.0 mg kg^{-1}; this quantity was reduced to 2,733.5 mg kg^{-1} when this mixture was combined with biostimulation (VCBS) and to 2,658.5 mg kg^{-1} when it was combined with bioaugmentation (VCBA). In this last case, the results revealed a moderate increase in EPHs degradation' efficiency when compared with samples without VC addition, reaching degradation rates of 10.1% (VCT), 32.5% (VCBS), and 34.4% (VCBA) of the initial hydrocarbon levels. Concerning the 16 EPA (Environmental Protection Agency) PAHs, Fig. 1B exhibits the scenario for the total PAHs fraction (left) per treatment at the end-point experiment (90 days). The concentration of the 16 EPA PAHs from the initial contaminated soil can be seen in Supplementary Table 1. However, a decreasing trend was

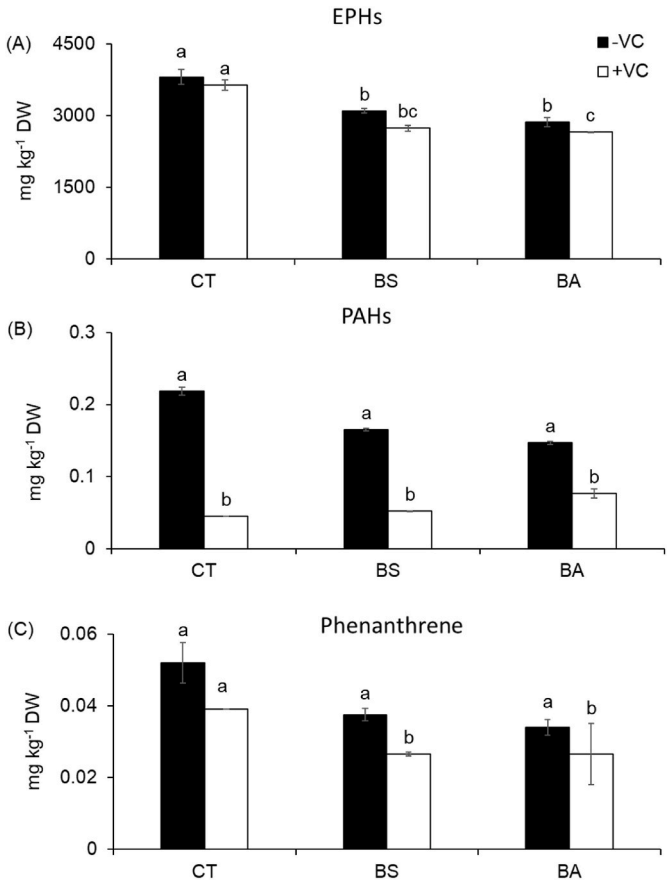

Fig. 1. (A) Content of Extractable Petroleum Hydrocarbons (EPHs) at the end of the 90 days incubation period; (B) Content of Polycyclic Aromatic Hydrocarbons (PAHs); and (C) phenanthrene at the end of the 90 days incubation period. Columns with different letters displayed significant statistical differences (one-way ANOVA, followed by Tukey's *post-hoc* test with significance defined at $p < 0.05$). DW: Dry Weight.

observed compared to the untreated control soil, either with or without VC addition. The results were not statistically significant. Specifically, the phenanthrene, the most abundant PAHs present in the soil understudy, was significantly reduced after the VCBS and VCBA treatments (Fig. 1B), from 0.052 mg kg^{-1} in the control soil to 0.0265 mg kg^{-1} in both treated soils (BS and BA).

It should be highlighted that, in this soil, EPHs corresponded to the TPHs fraction since the composition was dominated by medium and high molecular weight in both linear aliphatic and aromatic hydrocarbons (Figs. 2 and 3). In contrast, the volatile fraction was almost completely depleted, and this distribution did not change along with the 90-day incubation (CT). EPH fractions are displayed in different ranges as a function of the length of carbon chains and are shown in Fig. 2A and B for aliphatic and aromatic hydrocarbons, respectively. Aliphatic hydrocarbons (designated as Cn, where "n" is the number of C) in the ranges of C22–C35 and >C35 accounted for 79.4% of total EPHs content. For the aromatic hydrocarbons fraction (EC), EC22-EC35 and >EC35 accounted for another 15.0%. In the case of the aliphatic fraction, these long-chain hydrocarbons (C22–C35) represented the most degraded fraction during the incubation period and showed an apparent effect of soil microbial stimulation and inoculum addition while higher molecular weight hydrocarbons (>C35) were more recalcitrant against biodegradation. In the case of aromatic hydrocarbons, low molecular weight compounds (EC10-EC16) nearly disappeared in the treatments with vermicompost and microbial inoculation, whereas the highest molecular weight compounds displayed a similar pattern as described for aliphatic.

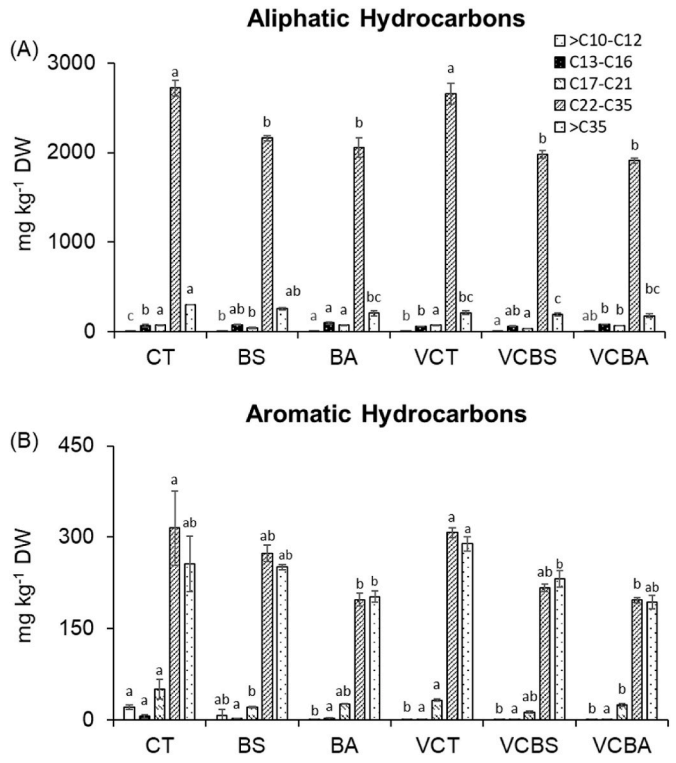

Fig. 2. Molecular ranges of EPH after liquid fractionation between aliphatic (A) and aromatic (B) hydrocarbons fractions at the end of the 90 days incubation period. Columns between fractions with different letters displayed significant statistical differences among treatments (One-way ANOVA, followed by Tukey's *post-hoc* test with significance defined at $p < 0.05$). DW: Dry Weight.

3.3. GC-MS qualitative study

Once the concentration of EPH and its fractions were evaluated as described above, a deeper examination of the evolution of the main hydrocarbon and non-hydrocarbon compounds was carried out utilizing a qualitative GC-MS (Gas Chromatography-Mass Spectrometry) study. The samples selected to compare the initial status and the advanced states of biodegradation were control (CT) and bioaugmentation with vermicompost (VCBA) after 60 days of incubation. As a first step, the fate of the main fractions of the contaminants was analyzed after LC fractionation according to the SARA procedure (Saturates, aromatics, resins, and asphaltenes). The F1 fraction (mainly aliphatics) was initially 22.8% of the total extract and rose to 36.7% after 60 days of incubation (VCBA treatment); a similar pattern was observed with the F2 fraction (mainly aromatics), which was increased from 4.3% to 5.9%; on the contrary, the sum of F3 fraction (polar compounds) and asphaltenes diminished from 72.8% to 57.4%. This initial result revealed that many polar compounds were degraded during the experiments (Fig. 3A and B). The predominant compounds within this polar F3 fraction were oleochemicals. Regarding the aliphatic fraction (F1), the main differences between CT and VCBA are shown in Fig. 3C (chromatograms in SIM –Single Ion Monitoring-mode m $z^{-1} = 57$) and Fig. 3D (SIM, m $z^{-1} = 191$).

In the chromatogram in Fig. 3C, the initial product displayed a fingerprint with a predominance of linear alkanes from 15 to 38 carbon atoms, enriched in heavy linear alkanes (with the maximum in 27 carbon atoms). It also shows a prevalence of linear alkanes over branched alkanes (n-C18 $Phytane^{-1}$ ratio slightly above 1) and a moderate UCM (Unresolved Complex Mixture), thereby revealing an initial moderate degradation and weathering of the hydrocarbons in soil. On the contrary, after 60 days of incubation in the VCBA treatment (Fig 3C), the linear alkanes were depleted entirely (n-C1 $Phytane^{-1} = 0$); branched

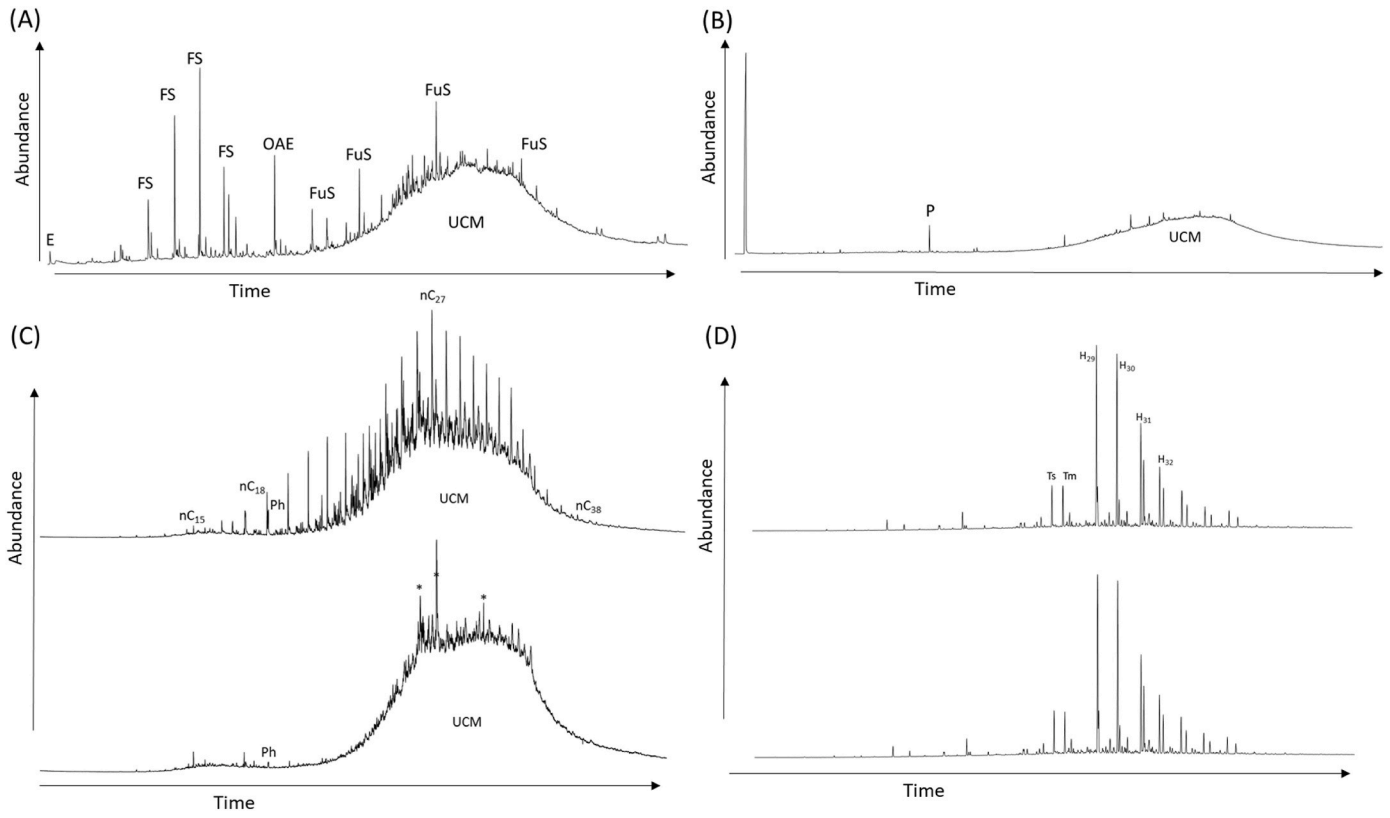

Fig. 3. Total Ion Chromatograms (TIC) represented in 3.A are 3.B are showing representative F3 fraction fingerprints, (A): CT control initial; (B): VCBA treatment after 60 days. Note that most of the compounds identified in the control (oleochemicals) were fully degraded after 60 days, this process was accompanied with a remarkable reduction of the UCM thereby revealing an almost complete depletion of fraction F3. *E: epoxioctane, FS: Fatty acid (saturated) esters; OAE: Oleic acid ester; PUFA: Fatty acid (unsaturated) esters; P: plasticizer; UCM: Unresolved Complex Mixture.* SIM (Single Ion Chromatograms) showing representative F1 fraction fingerprints of CT control initial (top) and VCBA treatment after 60 days (down). While 3.C. shows the SIM chromatograms (m z-1 = 57) of alkanes, and 3.D SIM chromatograms (m z-1 = 191) of hopanes. nCn: Linear alkanes of 'n' carbon atoms; Ph: Phytane (branched alkane); *: Other branched alkanes; Hx: Hopanes (x is the carbon number); Ts: 18α(H)-22,29,30-trisnorhopane; Tm: 17α(H)-22,29,30-trisnorhopane; UCM: Unresolved Complex Mixture.

alkanes such as isoprenoids, although less biodegradable, were also notably degraded (Phytane peak is almost negligible); the UCM is notable, and the predominant compounds were heavy branched alkanes, and mainly hopanes, a recalcitrant group of cycloalkanes that remained unaltered since the initial situation, as shown in Fig. 3D. Finally, although aromatics (fraction F2) were a minority fraction, alkylbenzenes were identified as the predominant compounds. As shown in Supplementary Fig. 1 (see Supplementary Material), after 60 days, a moderate reduction in the variety and abundance of these compounds was evidenced.

3.4. Changes in soil properties

The most significant results on the measured soil parameters and their evolution during the incubation strategies are displayed in Table 1. Soil pH values did not change significantly in the control soil (CT) during the whole incubation period; however, clear acidification was observed in the rest of the treatments, especially during the first 15 days. This acidification is associated with the introduction of inorganic and organic nutrients in the case of BS and VC treatments, respectively, and could be related to increased CO_2 production due to OM mineralization. The second inoculation (BA and VCBA) on day 43rd only provoked a slight decrease in the pH values on day 45th as compared with the control soil (CT) or the vermicompost-soil mixture (VCT).

Values of electrical conductivity (EC; Table 1) of the control soils, both with and without VC, displayed slight variations during the incubation. These values were lower than those observed for the samples subjected to biostimulation and bioaugmentation, reflecting the effect of nutrient additions. At the end of the incubation periods (before and after microbial consortia inoculation, i.e., days 0 and 43rd), a small drop in EC values was likewise observed due to the microbial consumption activity. Regarding the evolution of available P and K levels (Table 1), a different behavior was displayed compared to the EC parameter. In this case, the application of 2% vermicompost increased by more than five and two times the amounts of available orthophosphate (P-Olsen) and exchangeable-K, respectively, as a direct consequence of the organic amendment addition. The nutrient level increase was observed between BS-BA and VCBS-VCBA. These treatments presented the highest values of exchangeable-K and available orthophosphate throughout the whole incubation, except for day 45th, where the latter's levels reached similar values in all the treatments after the nutrient's addition.

Finally, the values of extractable organic C (EOC) and total extractable N (TEN), as a *proxy* to test the availability of C and N, are displayed in Table 2, respectively. Initial values of EOC were similar for all the treatments, being this particularly unusual in regolith soils, such is the case of the one used in this work, this being exclusively attributable to the presence of the soluble organic pollutants. For VCT samples, after an initial decrease in EOC observed during the first fifteen days, values remained consistently higher than in CT samples due to a probable priming effect of the incubation conditions. This increase in EOC was probably due to the depolymerization of macromolecules and the concomitant release of soluble low molecular weight compounds. This effect was also responsible for the higher values of EOC in BS and BA treatments, with and without VC addition. For TEN, a different situation was observed, where the initial depletion in this soil (CT) was noted even after the VC addition (Table 2). The low amount of VC added (2% w

Table 1
Impacts of applied treatments on the physio-chemical parameters of TPHs contaminated soil with reference to incubation intervals.

Treatments	Days	pH		EC		P		K	
		NV	V	NV	V	NV	V	NV	V
Control	2	7.58 ± 0.12 ^{ab}	7.62 ± 0.09 ^{a}	0.71 ± 0.04 ^{a}	0.68 ± 0.04 ^{c}	5.00 ± 0.74 ^{a*}	23.71 ± 3.37 ^{a*}	64.04 ± 1.84 ^{a*}	146.09 ± 5.20 ^{a*}
	15	7.53 ± 0.04 ^{b*}	6.77 ± 0.26 ^{d*}	0.73 ± 0.02 ^{a}	0.75 ± 0.02 ^{ab}	4.91 ± 0.30 ^{ab*}	18.09 ± 9.35 ^{ab*}	60.97 ± 0.76 ^{ab*}	133.09 ± 24.86 ^{a*}
	30	7.50 ± 0.00 ^{b*}	6.89 ± 0.03 ^{cd*}	0.74 ± 0.02 ^{a}	0.75 ± 0.03 ^{ab}	4.86 ± 0.11 ^{ab*}	19.34 ± 5.71 ^{ab*}	59.44 ± 1.91 ^{bc*}	131.12 ± 4.98 ^{a*}
	45	7.47 ± 0.04 ^{b*}	6.99 ± 0.41 ^{bc*}	0.75 ± 0.02 ^{a}	0.77 ± 0.01 ^{a}	4.82 ± 0.21 ^{ab*}	14.65 ± 5.04 ^{b*}	57.91 ± 3.12 ^{bc*}	137.23 ± 26.27 ^{a*}
	60	7.63 ± 0.08 ^{a*}	7.13 ± 0.17 ^{b*}	0.73 ± 0.06 ^{a}	0.73 ± 0.04 ^{ab}	4.60 ± 0.59 ^{ab*}	19.74 ± 1.06 ^{ab*}	60.30 ± 2.39 ^{bc*}	142.44 ± 6.30 ^{a*}
	90	7.67 ± 0.07 ^{a*}	7.01 ± 0.17 ^{b*}	0.71 ± 0.04 ^{a}	0.71 ± 0.04 ^{bc}	4.26 ± 0.20 ^{b*}	22.35 ± 2.59 ^{ab*}	56.81 ± 3.04 ^{c*}	143.54 ± 5.29 ^{a*}
Biostimulation	2	7.12 ± 0.18 ^{a}	7.20 ± 0.03 ^{a}	1.22 ± 0.08 ^{c}	1.42 ± 0.13 ^{b}	30.68 ± 7.58 ^{b*}	56.11 ± 4.58 ^{c*}	227.28 ± 36.96 ^{c*}	358.85 ± 34.63 ^{c*}
	15	6.58 ± 0.06 ^{c}	6.58 ± 0.08 ^{d}	1.30 ± 0.05 ^{c}	1.41 ± 0.08 ^{b}	25.35 ± 0.85 ^{b*}	40.79 ± 3.88 ^{d*}	243.48 ± 12.46 ^{c*}	333.04 ± 11.71 ^{c*}
	30	6.78 ± 0.09 ^{b}	6.74 ± 0.05 ^{c}	1.31 ± 0.05 ^{c}	1.36 ± 0.05 ^{b}	24.44 ± 2.24 ^{b*}	45.67 ± 4.39 ^{cd*}	254.41 ± 18.00 ^{c*}	317.32 ± 13.14 ^{c*}
	45	6.80 ± 0.05 ^{b}	6.84 ± 0.05 ^{b}	1.89 ± 0.16 ^{a}	1.88 ± 0.16 ^{a}	40.73 ± 7.00 ^{a*}	87.02 ± 18.65 ^{a*}	320.27 ± 26.98 ^{b*}	488.77 ± 47.90 ^{a*}
	60	7.11 ± 0.04 ^{a}	7.25 ± 0.04 ^{a}	1.73 ± 0.12 ^{b}	1.92 ± 0.10 ^{a}	47.14 ± 5.58 ^{a*}	97.91 ± 7.52 ^{a*}	353.84 ± 9.75 ^{a*}	471.78 ± 11.98 ^{ab*}
	90	6.99 ± 0.07 ^{a*}	7.19 ± 0.06 ^{a*}	1.74 ± 0.04 ^{b}	1.78 ± 0.08 ^{a}	47.80 ± 5.04 ^{a*}	72.46 ± 10.51 ^{b*}	358.04 ± 5.98 ^{a*}	429.09 ± 32.84 ^{b*}
Bioaugmentation	2	7.31 ± 0.10 ^{a}	7.18 ± 0.06 ^{a}	1.28 ± 0.03 ^{c}	1.46 ± 0.04 ^{b}	30.15 ± 4.82 ^{c*}	76.81 ± 13.32 ^{a*}	241.49 ± 10.33 ^{c*}	375.27 ± 21.28 ^{b*}
	15	6.60 ± 0.04 ^{e}	6.56 ± 0.02 ^{e}	1.30 ± 0.09 ^{c}	1.44 ± 0.06 ^{b}	21.39 ± 0.51 ^{d*}	57.27 ± 8.81 ^{b*}	246.51 ± 11.34 ^{c*}	369.36 ± 36.56 ^{b*}
	30	6.84 ± 0.04 ^{d}	6.73 ± 0.02 ^{d}	1.19 ± 0.04 ^{c}	1.27 ± 0.07 ^{b}	26.59 ± 3.74 ^{cd*}	48.02 ± 7.88 ^{b*}	238.56 ± 10.50 ^{c*}	327.96 ± 21.54 ^{c*}
	45	6.86 ± 0.03 ^{d}	6.87 ± 0.06 ^{c}	1.68 ± 0.02 ^{b}	1.99 ± 0.31 ^{a}	45.90 ± 3.50 ^{b*}	77.83 ± 5.64 ^{a*}	349.68 ± 20.52 ^{ab*}	496.97 ± 30.30 ^{a*}
	60	7.18 ± 0.05 ^{b}	7.19 ± 0.04 ^{a}	1.85 ± 0.10 ^{a}	2.01 ± 0.12 ^{a}	58.32 ± 4.09 ^{a*}	74.31 ± 5.40 ^{a*}	372.32 ± 13.64 ^{a*}	497.39 ± 28.45 ^{a*}
	90	7.10 ± 0.01 ^{c}	7.07 ± 0.03 ^{b}	1.70 ± 0.10 ^{b}	1.85 ± 0.09 ^{a}	47.70 ± 5.61 ^{b*}	74.49 ± 2.13 ^{a*}	344.22 ± 26.27 ^{b*}	521.36 ± 17.45 ^{a*}

Table 2
Impacts of applied treatments and incubation on extractable organic carbon and nitrogen, and basal soil respiration of TPHs contaminated soil.

Treatments	Days	EOC[1]		TEN[1]		BSR[1]	
		NV	V	NV	V	NV	V
Control	2	2341.17 ± 114.24 ^{a}	2331.01 ± 71.94 ^{c}	27.82 ± 0.22 ^{b*}	81.18 ± 3.22 ^{a*}	0.54 ± 4.29 ^{b}	0.69 ± 0.19 ^{c}
	15	2249.15 ± 61.17 ^{ab}	2119.95 ± 47.94 ^{c}	22.66 ± 0.19 ^{c*}	44.31 ± 1.22 ^{b*}	0.50 ± 2.02 ^{b*}	2.48 ± 0.34 ^{a*}
	30	2203.14 ± 40.09 ^{b}	2429.45 ± 67.73 ^{b}	20.08 ± 0.17 ^{cd*}	44.95 ± 5.84 ^{b*}	0.48 ± 0.95 ^{b*}	2.33 ± 0.13 ^{a*}
	45	2157.13 ± 33.94 ^{b*}	2491.95 ± 74.60 ^{ab*}	17.50 ± 0.16 ^{e*}	46.65 ± 4.39 ^{b*}	0.46 ± 0.59 ^{b*}	2.15 ± 0.22 ^{a*}
	60	2217.72 ± 97.37 ^{b*}	2561.68 ± 46.40 ^{a*}	33.94 ± 0.28 ^{a*}	47.15 ± 2.57 ^{b*}	1.03 ± 5.30 ^{a*}	2.19 ± 0.17 ^{a*}
	90	2347.32 ± 23.10 ^{a*}	2584.86 ± 62.42 ^{a*}	27.22 ± 1.84 ^{b*}	43.58 ± 3.22 ^{b*}	0.78 ± 0.26 ^{ab*}	1.77 ± 0.31 ^{b*}
Biostimulation	2	2357.27 ± 83.24 ^{c}	2473.96 ± 94.53 ^{d}	1024.04 ± 86.34 ^{b*}	839.28 ± 78.49 ^{b*}	0.33 ± 0.09 ^{e}	0.44 ± 0.03 ^{d}
	15	2474.22 ± 32.05 ^{c}	2389.59 ± 27.68 ^{d}	841.40 ± 27.66 ^{c*}	703.40 ± 57.20 ^{c*}	17.64 ± 1.15 ^{a*}	21.74 ± 1.28 ^{a*}
	30	3157.26 ± 168.32 ^{b}	2750.79 ± 56.56 ^{c}	710.18 ± 18.727 ^{d*}	575.01 ± 33.52 ^{d*}	4.26 ± 0.15 ^{b}	5.52 ± 0.29 ^{b}
	45	3155.56 ± 123.73 ^{b}	3009.84 ± 112.01 ^{b}	1198.54 ± 42.41 ^{a*}	1049.34 ± 37.74 ^{a*}	3.16 ± 0.13 ^{c}	3.20 ± 0.87 ^{c}
	60	3353.40 ± 89.55 ^{a}	3150.14 ± 113.78 ^{b}	1256.01 ± 8.33 ^{a*}	1073.69 ± 64.19 ^{a*}	2.47 ± 0.27 ^{d}	2.31 ± 0.13 ^{c}
	90	3339.97 ± 82.55 ^{a}	3333.55 ± 154.72 ^{a}	1236.03 ± 37.18 ^{a*}	1069.01 ± 72.47 ^{a*}	1.77 ± 0.16 ^{d}	2.45 ± 0.59 ^{c}
Bioaugmentation	2	2197.27 ± 59.66 ^{d*}	2532.44 ± 55.81 ^{c*}	961.51 ± 0.25 ^{b}	943.95 ± 91.14 ^{b}	0.79 ± 0.25 ^{f}	0.46 ± 0.26 ^{e}
	15	2576.80 ± 77.08 ^{c}	2555.47 ± 113.93 ^{c}	789.35 ± 0.33 ^{c}	774.34 ± 50.16 ^{c}	17.84 ± 0.33 ^{a}	17.36 ± 1.31 ^{a}
	30	2696.98 ± 57.38 ^{b*}	3029.71 ± 106.40 ^{b*}	651.44 ± 0.29 ^{d}	545.06 ± 68.58 ^{d}	4.31 ± 0.28 ^{b}	5.19 ± 0.17 ^{b}
	45	2666.36 ± 40.4 ^{b*}	3126.37 ± 121.71 ^{ab*}	1194.71 ± 0.01 ^{a}	1132.01 ± 157.01 ^{a}	2.88 ± 0.01 ^{c}	3.84 ± 0.32 ^{c}
	60	2909.94 ± 29.08 ^{a*}	3260.97 ± 106.02 ^{a*}	1219.05 ± 0.24 ^{a}	1234.27 ± 101.89 ^{a}	2.47 ± 0.23 ^{d}	2.46 ± 0.45 ^{d}
	90	2926.73 ± 52.63 ^{a*}	3258.03 ± 94.61 ^{a*}	1164.64 ± 0.27 ^{a}	1230.02 ± 95.09 ^{a}	1.57 ± 0.26 ^{e}	1.64 ± 0.12 ^{d}

w^{-1}), and its stability implied that most N was in organic forms, which is difficult to extract or quickly assimilated by soil biota. In contrast, the introduction of nutrient solutions was reflected in an initial increase of TEN, rapidly consumed during the first 30 days of incubation, showing a reduction of more than 30% in contrast to their initial contents. This effect disappeared after adding the second nutrient, revealing the inefficiency of introducing this surplus of nutrients in future experiments (Table 2).

3.5. Evolution of biological parameters

In order to complement and correlate the above-mentioned quantitative results on contaminants' degradation efficiency and soil parameters evolution, Basal Soil Respiration (BSR), enzyme profile activity, and PLFAs evolution were carefully analyzed. During the first incubation (2nd day), all the samples displayed very low BSR values. In control samples (CT), these values remained constant during the whole

incubation period, exhibiting a small increase only on day 45th, associated with the increase in soil humidity applied to reach 50% of the HWRC (Table 2). In contrast, the rest of the treatments evinced a substantial increase in BSR on day 15th, where VCBS samples displayed the highest values (nearly 50 times higher than the initial value), being growth lower for VCT (5 times higher than the initial value). The assimilation of the nutrients and the degradation of the most labile organic fractions, probably including low molecular weight aliphatic and aromatic hydrocarbons, could be associated with the increased values encountered for this parameter. On the other hand, despite the substantial increment in nutrients, such as the associated release of available N, P, and K, the second inoculation or nutrient addition was only responsible for a limited rise in BSR. The absence of labile organic fractions to support the microbial activity of a microbial consortium specialized in diesel degradation, as in the current study, could explain the observed lack of microbial growth.

The evolution of soil microbial activity is complemented by assessing the evolution of the enzymatic activity profile for the samples at four different times: 2, 15, 45, and 90 days. The results are presented in Table 3. After 2 days of incubation, the soil enzyme profile for the control soil reflected the lowest microbial activity in the polluted soil. This profile did not significatively vary with the addition of the microbial consortium, but more significant changes were observed for BS and the samples with VC. In these samples, all activities were increased, mainly phosphatases (alkPA but also AcPA), chitinases (bNAG), and proteases (LeuAMP), which supposed an increase in their catabolic capacities. This feature was maintained on day 15th, where a general increase in all the enzyme profiles was observed, and it definitively changed on day 45th, after the second inoculation. At this time, a marked increase of bNAG and, to a lesser extent, in bGA (mainly for BA, BS, and VCBA samples) was observed. This enzyme profile was also observed at 90 days of incubation, except for AlkPA and bNAG activities, which showed a lower trend. This substantial increase of bNAG, one of the enzymes involved in the final process of chitin degradation, could be associated with the initial and severe fungal development observed during the first 15 incubation days and considering that the mycelia were mixed with the soil during the periodic soil aerations of microcosms (Table 3).

The analysis of PLFAs, as an indirect determination of the soil microbial biomass, was carried out at 15 and 90 days of incubation. According to BSR results (Table 2) and the final composition of the bioremediation mixtures, these time points were selected as representatives of the highest picks in microbial activity. The results for total PLFAs (Fig. 4A) reflect a trend of the microbial biomass from the initial moments of the incubation, in which samples with vermicompost displayed the highest values of microbial biomass till the end of the incubation when BS and BA exhibited higher microbial numbers than the rest of the treatments. Comparing the different bacterial microbial groups (Fig. 4B, C, and D), Gram-positive bacteria (Fig. 4C) were predominant, with a higher prevalence in VCBA and VCBS at the beginning of the experience (15 days). On the contrary, for Gram-negative bacteria (Fig. 4D) and actinobacteria (Fig. 4E), results displayed higher values at the end of the experience than at the beginning in most of the cases, reflecting the changes in the microbial community happening along the incubation process, as a consequence of nutrient, consortium, and vermicompost additions. Fungal components (Fig. 4F) were higher in both BA and VCBA samples than in each respective control on day 15th; this proportion was the opposite at the end of the experience when a higher presence of these fungal components was observed in BA and BS samples.

4. Discussion

Traditionally, three bioremediation strategies for TPHs pollution have been used: natural attenuation, biostimulation, and bioaugmentation (Khan et al., 2016b; Hussain et al., 2022). Natural

Table 3
Enzymatic profile of TPHs containment soil with different applied treatments and incubation durations.

Treatments	Days	Control		Biostimulation		Bioaugmentation	
		NV	V	NV	V	NV	V
Acid phosphatase	0	13.56 ± 0.28 ^{a*}	71.76 ± 1.49 ^{a*}	23.02 ± 0.48 ^{a*}	72.13 ± 1.49 ^{a*}	20.49 ± 0.42 ^{c*}	85.52 ± 3.54 ^{a*}
	15	10.53 ± 2.04 ^{ab*}	90.24 ± 17.95 ^{a*}	22.2 ± 4.31 ^{a*}	66.83 ± 18.17 ^{a*}	43.04 ± 10.65 ^{a*}	83.02 ± 23.04 ^{a*}
	45	7.49 ± 3.98 ^{c*}	69.65 ± 10.2 ^{a*}	17.62 ± 1.62 ^{a*}	67.06 ± 28.5 ^{a*}	27.51 ± 16.47 ^{ab*}	48.07 ± 14.18 ^{b*}
	90	11.23 ± 5.32 ^{ab*}	72.6 ± 43.46 ^{a*}	25.44 ± 11.04 ^{a*}	62.67 ± 30.47 ^{a*}	13.3 ± 4.87 ^{c*}	55.06 ± 22.97 ^{b*}
α-glucosidase	0	1.43 ± 0.03 ^{c*}	17.82 ± 0.37 ^{c*}	2.36 ± 0.05 ^{b}	14.99 ± 0.31 ^{c*}	3.15 ± 0.07 ^{c*}	11.50 ± 0.48 ^{b*}
	15	5.05 ± 2.05 ^{bc*}	108.12 ± 15.87 ^{a*}	39.77 ± 1.72 ^{b}	106.21 ± 19.84 ^{b*}	89.43 ± 21.06 ^{b*}	170.55 ± 46.85 ^{a*}
	45	8.66 ± 4.09 ^{b*}	60.45 ± 13.65 ^{b*}	152.49 ± 23.76 ^{a}	203.96 ± 48.55 ^{a*}	132.05 ± 38.19 ^{a*}	188.9 ± 72.62 ^{a*}
	90	16.87 ± 6.17 ^{a*}	47.2 ± 10.72 ^{b*}	143.29 ± 82.21 ^{a}	146.94 ± 41.37 ^{b}	126.13 ± 16.61 ^{a*}	196.65 ± 24.64 ^{a*}
β-glucosidase	0	0.87 ± 0.03 ^{b*}	3.91 ± 0.08 ^{c*}	2.59 ± 0.46 ^{a*}	4.57 ± 0.09 ^{a*}	2.78 ± 0.06 ^{a}	2.42 ± 0.10 ^{a}
	15	0.89 ± 0.03 ^{b*}	4.22 ± 0.64 ^{c*}	2.65 ± 0.47 ^{a*}	3.57 ± 0.79 ^{a*}	1.92 ± 0.86 ^{a*}	5.14 ± 2.91 ^{a*}
	45	1.77 ± 0.05 ^{a*}	6.64 ± 2.06 ^{b*}	2.56 ± 0.47 ^{a*}	4.93 ± 1.98 ^{a*}	1.61 ± 0.51 ^{a*}	3.38 ± 1.58 ^{a*}
	90	1.39 ± 0.69 ^{ab*}	10.64 ± 1.51 ^{a*}	2.49 ± 1.11 ^{a*}	4.68 ± 1.88 ^{a*}	1.79 ± 0.21 ^{a*}	4.18 ± 1.27 ^{a*}
β-xylosidase	0	0.43 ± 0.01 ^{a*}	5.89 ± 0.12 ^{c*}	1.19 ± 0.02 c*	7.98 ± 0.17 ^{b*}	4.23 ± 0.09 ^{b}	4.51 ± 0.19 ^{c}
	15	1.05 ± 0.66 ^{a*}	12.64 ± 1.09 ^{a*}	9.11 ± 2.06 ^{b*}	20.95 ± 5.45 ^{a*}	11.08 ± 2.34 ^{a*}	26.14 ± 6.21 ^{a*}
	45	1.67 ± 1.31 ^{a*}	10.34 ± 3.12 ^{ab*}	13.25 ± 1.36 ^{a*}	20.49 ± 3.29 ^{a*}	11.02 ± 2.16 ^{a*}	19.73 ± 7.14 ^{ab*}
	90	2.34 ± 1.12 ^{a*}	9.28 ± 1.68 ^{b*}	9.62 ± 4.4 ^{ab}	12.36 ± 2.75 ^{b}	8.90 ± 2.83 ^{a*}	12.55 ± 2.68 c*
N-acetyl-β-glucosaminidase	0	2.86 ± 0.06 ^{b*}	26.36 ± 0.55 ^{b*}	2.59 ± 0.05 ^{b*}	19.48 ± 0.40 ^{n*}	5.60 ± 0.12 ^{c*}	15.47 ± 0.64 ^{c*}
	15	13.38 ± 8.42 ^{b*}	161.91 ± 11.38 ^{a*}	51.24 ± 20.98 ^{b}	44.18 ± 22.87 ^{b}	159.36 ± 30.54 ^{b*}	137.43 ± 76.32 ^{b*}
	45	23.9 ± 16.83 ^{b*}	127.66 ± 33.69 ^{a*}	553.91 ± 59.10 ^{a*}	307.25 ± 137.39 ^{a*}	621.91 ± 112.39 ^{a*}	293.44 ± 71.72 ^{b*}
	90	90.1 ± 37.01 ^{a*}	138.71 ± 35.07 ^{a*}	466.27 ± 190.45 ^{*a}	316.96 ± 116.45 ^{a*}	537.67 ± 94.66 ^{a*}	419.85 ± 53.38 ^{a*}
Sulfatase	0	0.65 ± 0.03 ^{b*}	3.71 ± 0.08 ^{a*}	1.54 ± 0.27 ^{a*}	4.71 ± 0.10 ^{a*}	2.66 ± 0.06 ^{a}	2.91 ± 0.12 ^{a}
	15	0.67 ± 0.03 ^{b*}	3.93 ± 0.55 ^{a*}	1.59 ± 0.27 ^{a*}	3.12 ± 0.63 ^{a*}	1.12 ± 0.89 ^{b}	2.48 ± 1.17 ^{a}
	45	1.33 ± 0.06 ^{a*}	4.45 ± 0.99 ^{a*}	1.60 ± 0.65 ^{a*}	4.04 ± 1.64 ^{a*}	1.32 ± 0.24 ^{b*}	2.61 ± 1.40 ^{a*}
	90	0.26 ± 0.19 ^{c*}	3.44 ± 1.42 ^{a*}	1.61 ± 0.92 ^{a*}	4.36 ± 1.70 ^{a*}	1.02 ± 0.17 ^{b*}	3.56 ± 1.13 ^{a*}
Alkaline phosphatase	0	8.99 ± 0.19 ^{b*}	179.2 ± 3.71 ^{b*}	31.32 ± 0.65 ^{b*}	42.44 ± 0.88 ^{b*}	12.18 ± 0.25 ^{b*}	66.80 ± 2.77 ^{c}
	15	50.95 ± 35.37 ^{*a}	341.46 ± 105.24 ^{a*}	93.02 ± 45.41 ^{ab*}	125.54 ± 28.58 ^{a*}	251.38 ± 115.58 ^{a}	248.44 ± 74.54 ^{a}
	45	92.90 ± 70.6 ^{a*}	489.12 ± 109.78 ^{a*}	92.53 ± 8.49 ^{ab*}	164.42 ± 62.07 ^{a*}	226.97 ± 124.81 ^{a*}	161.93 ± 54.41 ^{ab*}
	90	64.82 ± 20.74 ^{a*}	372.87 ± 144.3 ^{a*}	178.24 ± 103.45 ^{a}	153.78 ± 35.42 ^{a}	76.41 ± 15.14 ^{ab*}	246.5 ± 78.89 ^{a*}
Leucine aminopeptidase	0	7.48 ± 0.15 ^{a*}	15.44 ± 0.32 ^{b*}	31.29 ± 0.65 ^{a*}	13.34 ± 3.28 ^{a*}	6.96 ± 0.14 ^{c*}	17.9 ± 0.74 ^{a*}
	15	7.35 ± 0.43 ^{a*}	34.68 ± 4.65 ^{a*}	17.54 ± 6.84 ^{b*}	25.35 ± 6.88 ^{a*}	30.16 ± 7.27 ^{a}	30.69 ± 16.47 ^{a}
	45	7.23 ± 0.86 ^{a*}	38.70 ± 15.2 ^{a*}	17.60 ± 2.86 ^{b}	19.22 ± 6.86 ^{a}	21.24 ± 6.94 ^{b}	16.41 ± 7.67 ^{a}
	90	7.82 ± 4.18 ^{a*}	26.81 ± 6.96 ^{ab*}	16.83 ± 6.77 ^{b}	22.38 ± 5.57 ^{a}	15.83 ± 4.76 ^{b}	21.38 ± 11.44 ^{a}

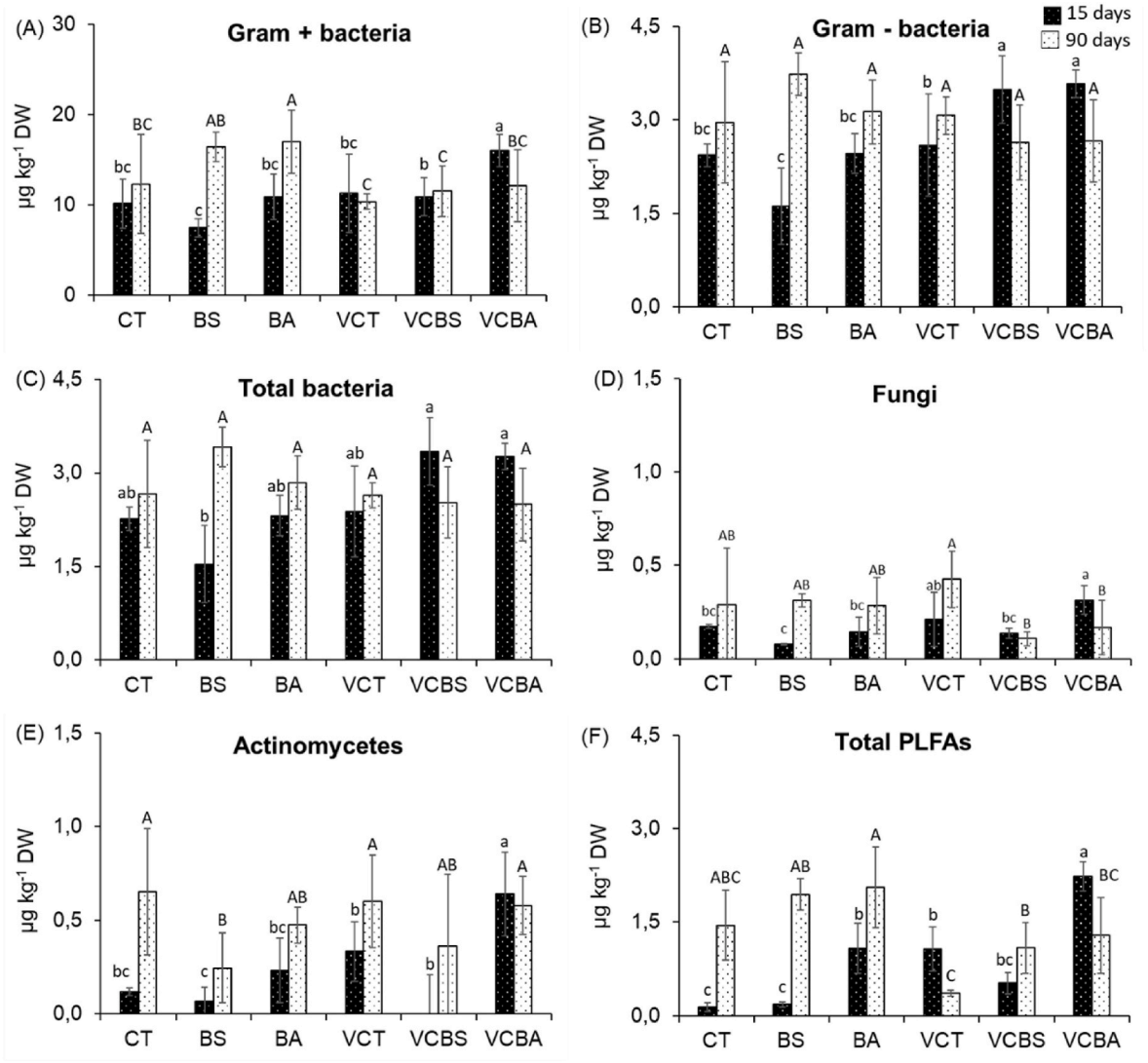

Fig. 4. Changes in soil microbial community measured using PLFAs as biomarkers: (A) Gram + bacteria, (B) Gram-bacteria, (C) Total bacteria, (D) Fungi, (E) actinomycetes and (F) Total PLFAs. Different letters (capital and small letters, for 15 and 90 days, respectively) displayed significant statistical differences between treatments at the two incubation times (15 and 90 days). One-way ANOVA, followed by Tukey's *post-hoc* test with significance defined at $p < 0.05$. DW: Dry Weight.

attenuation, one of the most straightforward ways to treat soil pollution, uses the intrinsic degradation capability of the autochthonous microorganisms to degrade contaminants; however, it has a long period to achieve successful results due to the low population size of indigenous degrading microorganisms, or the adverse soil physical-chemical conditions (Yousaf et al., 2022). In the present study, control samples did not significantly change TPHs concentrations, neither aliphatic nor aromatic fractions, even though soil incubation was carried out under optimal temperature, aeration, and available water for microbial growth. It illustrates the real and limiting possibilities of natural attenuation and the boundaries of its implementation to decrease TPHs' concentration below the established threshold values for polluted soils. In our case, TPHs remained 100 times over the values of generic reference levels, according to the Spanish legislation (Pinedo et al., 2013). PAHs were reduced, especially in the case of the most abundant compound detected in the sample, the phenanthrene, whose decrease was statistically significant both in VCBS and VCBA treatments in the presence of vermicompost, indicating the possible adsorption and sequestration mechanisms occurring in the matrix of the organic amendment mixed with the soil. Although more results are needed to understand PAHs alleviation in soils via bioremediation, this problem was not the main challenge to address in the current study since the original PAHs values were not high in terms of toxicity and threshold limits.

The polluted soil used in this experience is a regolith more than a proper soil, as it is comprised of pickling layers of surface soils affected by diesel and oil spills in a machinery park. Organic matter was close to 4%, comprising the targeted organic pollutants and, consequently, is challenging to use as substrates for microbial growth. The contents of other vital nutrients, such as N or P, are depleted in this soil. Applying a BHB-culture media had a clear response in activating microbial activity. It was reflected in the increase in BSR observed in the BS treatment after 15 days of incubation. This increased microbial activity was also reflected in the soil enzyme profile, which displayed an increment in the activity of the APA and proteases, clearly linked to bacterial growth in the first days of the incubation period. The stimulation of microbial metabolism was correlated with the observed degradation of TPHs.

In this work, a consortium isolated from the polluted soil was grown in a culture media in which diesel oil was added as a sole carbon source. The isolated consortium had similar features to a previously isolated consortium from another diesel-polluted soil (Garrido-Sanz et al., 2019), and its microbiome was dominated by bacterial species of the genus *Pseudomonas*, *Achromobacter*, *Cupriavidus*, *Comamonadaceae,* and *Sphingomonadaceae*. Metagenomic data identified redundant genes encoding enzymes implicated in the initial oxidation of alkanes: *alkane*

1-monooxygenase (*AlkB*), *long-chain alkane monooxygenase* (*LadA*), *cytochrome P450 alkane hydrolase* (*CYP153* family), and a variety of *hydroxylating and ring-cleavage dioxygenases*, involved in aromatic and polyaromatic hydrocarbon degradation that assured an efficient degradation of complex mixtures, such our polluted soil (Garrido-Sanz et al., 2019). Our results displayed an increase in the degradation capacity of TPHs promoted by the specific microbial enrichment of the polluted soil. However, this was insufficient to degrade high molecular weight aliphatic and aromatic hydrocarbons. The immobilization of recalcitrant TPHs, such as branched aliphatic, PAHs and substituted aromatic hydrocarbons on some soil constituents like mineral clays or humified organic materials, reducing their bioavailability to soil microorganisms, is a critical limiting factor in the bioremediation of an aged and polluted soil (Hussain et al., 2022).

In the present study, the microbial activity increased after compost and nutrient addition due to acidification of soil solution, resulting in more than one pH unit variation, which seems to be responsible for an essential effect in the solubility of P and other micronutrients and the predominance of different microbial groups. However, the second inoculation had a lower effect on soil respiration and nutrient consumption such as N and P. Many studies have already reported the effectiveness of bioaugmentation with microorganisms, either individually or in a consortium (Wu et al., 2017). However, adding different microbial communities does not always have an additive effect, and sometimes, microbial competition for soil resources or changes in nutrients' ratio (C:N:P) leads to microbial inhibition (Hussain el at., 2022; Khan et al., 2016ab). Degradation of hydrocarbons is often the result of a community-interacting microbial population, either structurally or functionally, and bioremediation's potential depends on these organisms' ability to adapt to new environmental conditions (Mishra et al., 2021). In this work, bioaugmentation and biostimulation increased soil TPHs' degradation capacity. Nevertheless, no statistically significant differences were observed with the biostimulation treatments either with or without vermicompost addition. A second inoculation or nutrient addition on day 43rd of the incubation did neither display an apparent effect in soil microbial activity; accordingly, it seemed like the second introduction of nutrients would be unnecessary with an evident accumulation of some of them, such as N and P.

A comprehensive understanding of how bioremediation influences the diversity of the soil microbial community is key to getting better insights into the behavior and function of these populations and correlating this with pollutants degradation in every situation (Narendrula-Kotha and Nkongolo, 2017). PLFAs were used as valuable viable or active microbial biomass biomarkers in our study. These are membrane lipids rapidly metabolized and decomposed outside the cell, as demonstrated by (Lewe et al., 2021). The functional adaptation of the soil microbial community reflected in the dynamics of individual hydrocarbons was mirrored by structural adaptation reflected in PLFA dynamics expressed by a site-specific PFLA ratio (Narendrula-Kotha and Nkongolo, 2017). Mair et al. (2013) reflected the correlation between PLFA determinations and TPH degradation in a hydrocarbon-contaminated soil from an Alpine former military site, testing the effects of temperature and biostimulation. Their data demonstrated the suitability of PLFA analysis for profiling microbial communities in hydrocarbon-contaminated soils. Chen et al. (2015) showed that temperature significantly influenced fungal to bacterial PLFA ratios and Gram-positive to Gram-negative bacterial ratios in pyrene-contaminated soil bioremediation with compost. The PLFA pattern in several pans of a site contaminated with PAHs, in which landfarming with biostimulation and bioaugmentation was tested, also evinced the enhancement of Gram-negative *Pseudomonas* spp. at the end of the experience (George and Wan, 2020). Gram-positive bacteria were predominant in the current study, with a higher amount present in the treatment with vermicompost (VCBA and VCBS) at the beginning of the experience (15 days). Whereas fungal components were initially higher in both BA and VCBA, the trend changed at the end of the incubation, as fungal PLFAs increased in BS and VCBS. Gram-negative bacteria and actinobacteria groups were mainly in higher abundance at the end of the experience. Again, these results prove the variations of the microbial community's predominant groups in every situation. It depends on the treatment and remediation time. Petroleum components are classified into bulk groups of saturates, olefins, aromatics, resin (including a wide variety of compounds containing sulfur, oxygen, and nitrogen), and asphaltenes. Initial contamination presented a profile enriched in heavy linear alkanes suggesting a previous moderate weathering (Gallego et al., 2011). The SARA fractionation procedure is commonly used to identify which fractions of the polluted soil are degraded during the remediation experience. Despite the good microbial growth in respiration, enzymatic activity stimulation, and nutrient consumption, results suggested that recalcitrant and hydrophobic petroleum compounds remained unchanged, revealing that mobility is linked to the bioavailability of these pollutants, the probable limiting step for soil recovery. The GC-MS study revealed a typical fingerprint of lubricant oils (Yang et al., 2016), including a mixture of aged hydrocarbons. Polar fractions, mainly composed of non-hydrocarbon oleochemicals, were in coherence with the activities in the study site (machinery park area) and rapidly consumed along with the experiments. Similar findings were reported by Soni and Agarwal (2014). Also, linear alkanes were depleted entirely, whereas branched alkanes such as isoprenoids and aromatics were moderately degraded in coherence with the reduction of medium-weight hydrocarbons observed in the quantitative study (Fig. 2). Consequently, the predominant compounds were hopanes after the treatments, a recalcitrant heavy-weight group of cycloalkanes typically abundant in severely weathered and biodegraded samples (Gallego et al., 2011). Finally, volatilization and similar abiotic degradation and removal mechanisms can be discarded to have occurred during the microcosm incubations.

A comprehensive study focusing on understanding the specific microbial species, biomass changes, and interactions involved in soil microbial remediation will be very interesting in identifying the potential functional microbial community. One such study was performed by Garrido-Sanz et al. (2019), in which they isolated and characterized the indigenous soil aerobic bacterial consortium growing on diesel as a sole carbon source. Garrido-Sanz et al. (2019) identified that the microbial consortium, using metagenomic analysis, capable of degrading hydrocarbon was primarily composed of *Pseudomonas, Aquabacterium, Chryseobacterium,* and *Sphingomonadaceae*. It is proposed that further research is needed for a better and more comprehensive understanding of the underlying mechanism of both BS and BA and to make better and more accurate informed decisions on implementing a given bioremediation strategy by considering not only the environment but also the rest of the inherent factors. While biostimulation might, in principle, result in better cost-effective options since the stage of cultivation of microorganisms is not necessary, more promising effects are a priori assigned when observing bioaugmentation results, mainly concerning the rate and time of degradation of HC, as derived from the current work.

5. Conclusions

In general lines, it can be stated that both strategies have had significant improvements, as observed in the biodegradation rates. After long-term *in situ* natural attenuations, the main biodegradable contaminant fractions were depleted. From that initial situation, the treatments applied were able to eliminate the remaining bioavailable compounds (linears, alkanes, and polars) and deplete fewer biodegradable compounds (aromatics and branched alkanes), whereas recalcitrant and heavy hydrocarbon families (hopanes) remained intact. Although there have been remarkable differences between and among the biostimulation and bioaugmentation treatments, most of them are not sufficiently significant to discriminate and select one over the other, for instance, in the case of upscaling the strategy (like for bio-pile). Significant differences were observed in the microcosms treatments with

the added vermicompost amendment, which can be a cost-effective technique to increase hydrocarbons' biodegradation when applied to large-scale bio-pile treatments. Similarly, using other co-application techniques also potentially speed up the hydrocarbon remediation process. These methods included the biofortification using microalgal biomass, amendments with soil conditioners, and other remediation methods (biosnorkeling, bioelectrokinesis, and mycoremediation). It will be interesting to study the evolution of microbial communities to design a functional hydrocarbon-degrading microbial pollution. Lastly, it will be important to quantify the level of soil toxicity followed by any remediation techniques adopted.

CRediT author statement

S. Curiel-Alegre: Methodology, Soil and lab analysis, initial draft preparation; B. Velasco-Arroyo: soil and lab analysis, initial draft preparation; C. Rumbo: microbial analysis; J.A. Tamayo-Ramos, A.H.A. Khan, C. Rad, and R. Barros: Conceptualization, text revision, and supervision. JL R. Gallego: GC-MS analysis and interpretation.

Funding sources

This work is funded by the GREENER project of the European Union's Horizon 2020 research and innovation program (Grant Agreement No. 826312). S. Curiel pre-doctoral contract was funded by Junta de Castilla y León (ORDEN EDU/1508/2020, de 15 de diciembre).

Declaration of competing interest

The authors declare that they have no known competing financial interests or personal relationships that could have appeared to influence the work reported in this paper.

Data availability

Data will be made available on request.

Acknowledgments

Authors are grateful to María Tomé and Andrea Martínez for their technical help in soil determinations and Azucena Martín for their lab assistance in TPHs determination. Authors are also thankful to Prof. Rafael Rivilla from Departamento de Biología, Facultad de Ciencias, Universidad Autónoma de Madrid, Madrid, Spain, for providing the isolated hydrocarbon-degrading bacterial consortium.

Appendix A. Supplementary data

Supplementary data to this article can be found online at https://doi.org/10.1016/j.chemosphere.2022.135638.

References

Bligh, E.G., Dyer, W.J., 1959. A rapid method of total lipid extraction and purification. Can. J. Biochem. Physiol. 37, 911–917. https://doi.org/10.1139/o59-099.

Chen, M., Xu, P., Zeng, G., Yang, C., Huang, D., Zhang, J., 2015. Bioremediation of soils contaminated with polycyclic aromatic hydrocarbons, petroleum, pesticides, chlorophenols and heavy metals by composting: applications, microbes and future research needs. Biotechnol. Adv. 33, 745–755. https://doi.org/10.1016/j.biotechadv.2015.05.003.

Das, D., Deka, H., 2021. Vermicomposting of harvested waste biomass of potato crop employing *Eisenia fetida*: changes in nutrient profile and assessment of the maturity of the end products. Environ. Sci. Pollut. Res. 28, 35717–35727. https://doi.org/10.1007/s11356-021-13214-z.

Gallego, J.L.R., Sierra, C., Permanyer, A., Peláez, A.I., Menéndez-Vega, D., Sánchez, J., 2011. Full-scale remediation of a jet fuel-contaminated soil: assessment of biodegradation, volatilisation, and bioavailability. Water, air. Soil Pollut. 217, 197–211. https://doi.org/10.1007/S11270-010-0579-6.

Garrido-Sanz, D., Redondo-Nieto, M., Guirado, M., Jiménez, O.P., Millán, R., Martin, M., Rivilla, R., 2019. Metagenomic insights into the bacterial functions of a diesel-degrading consortium for the rhizoremediation of diesel-polluted soil. Genes 10, 456. https://doi.org/10.3390/GENES10060456.

George, S.E., Wan, Y., 2020. Advances in characterizing microbial community change and resistance upon exposure to lead contamination: implications for ecological risk assessment. Crit. Rev. Environ. Sci. Technol. 50, 2223–2270. https://doi.org/10.1080/10643389.2019.1698260.

Hussain, F., Hussain, I., Khan, A.H.A., Muhammad, Y.S., Iqbal, M., Soja, G., Reichenauer, T.G., Yousaf, S., 2018. Combined application of biochar, compost, and bacterial consortia with Italian ryegrass enhanced phytoremediation of petroleum hydrocarbon contaminated soil. Environ. Exp. Bot. 153, 80–88. https://doi.org/10.1016/j.envexpbot.2018.05.012.

Hussain, F., Khan, A.H.A., Hussain, I., Farooqi, A., Muhammad, Y.S., Iqbal, M., Arslan, Yousaf, S., 2022. Soil conditioners improve rhizodegradation of aged petroleum hydrocarbons and enhance the growth of *Lolium multiflorum*. Environ. Sci. Pollut. Res. 29, 9097–9109. https://doi.org/10.1007/s11356-021-16149-7.

Iqbal, A., Mushtaq, M.U., Khan, A.H.A., Nawaz, I., Yousaf, S., Iqbal, M., 2020. Influence of *Pseudomonas japonica* and organic amendments on the growth and metal tolerance of *Celosia argentea* L. Environ. Sci. Pollut. Res. 27, 24671–24685. https://doi.org/10.1007/s11356-019-06181-z.

Khan, A.H.A., Anees, M., Arshad, M., Muhammad, Y.S., Iqbal, M., Yousaf, S., 2016b. Effects of illuminance and nutrients on bacterial photo-physiology of hydrocarbon degradation. Sci. Total Environ. 557, 705–711. https://doi.org/10.1016/j.scitotenv.2016.03.068.

Khan, A.H.A., Ayaz, M., Arshad, M., Yousaf, S., Khan, M.A., Anees, M., Sultan, A., Nawaz, I., Iqbal, M., 2019. Biogeochemical cycle, occurrence and biological treatments of polycyclic aromatic hydrocarbons (PAHs). Iran. J. Sci. Technol. Trans. Sci. 43, 1393–1410. https://doi.org/10.1007/s40995-017-0393-8.

Khan, A.H.A., Tanveer, S., Alia, S., Anees, M., Sultan, A., Iqbal, M., Yousaf, S., 2017. Role of nutrients in bacterial biosurfactant production and effect of biosurfactant production on petroleum hydrocarbon biodegradation. Ecol. Eng. 104, 158–164. https://doi.org/10.1016/j.ecoleng.2017.04.023.

Khan, A.H.A., Tanveer, S., Anees, M., Muhammad, Y.S., Iqbal, M., Yousaf, S., 2016a. Role of nutrients and illuminance in predicting the fate of fungal mediated petroleum hydrocarbon degradation and biomass production. J. Environ. Manag. 176, 54–60. https://doi.org/10.1016/j.jenvman.2016.03.040.

Lewe, N., Hermans, S., Lear, G., Kelly, L.T., Thomson-Laing, G., Weisbrod, B., Wood, S.A., Keyzers, R.A., Deslippe, J.R., 2021. Phospholipid fatty acid (PLFA) analysis as a tool to estimate absolute abundances from compositional 16S rRNA bacterial metabarcoding data. J. Microbiol. Methods 188, 106271. https://doi.org/10.1016/j.mimet.2021.106271.

Mair, J., Schinner, F., Margesin, R., 2013. A feasibility study on the bioremediation of hydrocarbon-contaminated soil from an Alpine former military site: effects of temperature and biostimulation. Cold Reg. Sci. Technol. 96, 122–128. https://doi.org/10.1016/j.coldregions.2013.07.006.

Marx, M.C., Wood, M., Jarvis, S.C., 2001. A microplate fluorimetric assay for the study of enzyme diversity in soils. Soil Biol. Biochem. 33, 1633–1640. https://doi.org/10.1016/S0038-0717(01)00079-7.

Mehlich, A., 1984. Mehlich 3 soil test extractant: a modification of Mehlich 2 extractant. Commun. Soil Sci. Plant Anal. 15, 1409–1416. https://doi.org/10.1080/00103628409367568.

Mishra, S., Lin, Z., Pang, S., Zhang, W., Bhatt, P., Chen, S., 2021. Recent advanced technologies for the characterization of xenobiotic-degrading microorganisms and microbial communities. Front. Bioeng. Biotechnol. 9, 632059 https://doi.org/10.3389/fbioe.2021.632059.

Mushtaq, M.U., Iqbal, A., Nawaz, I., Mirza, C.R., Yousaf, S., Farooq, G., Ali, M.A., Khan, A.H.A., Iqbal, M., 2020. Enhanced uptake of Cd, Cr, and Cu in *Catharanthus roseus* (L.) G. Don by *Bacillus cereus*: application of moss and compost to reduce metal availability. Environ. Sci. Pollut. Res. 27, 39807–39818. https://doi.org/10.1007/s11356-020-08839-5.

Narendrula-Kotha, R., Nkongolo, K.K., 2017. Bacterial and fungal community structure and diversity in a mining region under long-term metal exposure revealed by metagenomics sequencing. Ecol. Genet. Genom. 2, 13–24. https://doi.org/10.1016/j.egg.2016.11.001.

Palojärvi, A., 2006. Phospholipid fatty acid (PLFA) analyses. In: Bloem, J., Hopkins, D. W., Benedetti, A. (Eds.), Microbiological Methods for Assessing Soil Quality. CABI International, Wallingford, UK, pp. 204–211.

Pinedo, J., Ibáñez, R., Lijzen, J.P.A., Irabien, Á., 2013. Assessment of soil pollution based on total petroleum hydrocarbons and individual oil substances. J. Environ. Manag. 130, 72–79. https://doi.org/10.1016/J.JENVMAN.2013.08.048.

Sima, N.A.K., Ebadi, A., Reiahisamani, N., Rasekh, B., 2019. Bio-based remediation of petroleum-contaminated saline soils: challenges, the current state-of-the-art and prospects. J. Environ. Manag. 250, 109476 https://doi.org/10.1016/j.jenvman.2019.109476.

Soni, S., Agarwal, M., 2014. Lubricants from renewable energy sources – a review. Green Chem. Lett. Rev. 7, 359–382. https://doi.org/10.1080/17518253.2014.959565.

Wu, M., Li, W., Dick, W.A., Ye, X., Chen, K., Kost, D., Chen, L., 2017. Bioremediation of hydrocarbon degradation in a petroleum-contaminated soil and microbial population and activity determination. Chemosphere 169, 124–130. https://doi.org/10.1016/J.CHEMOSPHERE.2016.11.059.

Yang, C., Yang, Z., Zhang, G., Hollebone, B., Landriault, M., Wang, Z., Lambert, P., Brown, C.E., 2016. Characterization and differentiation of chemical fingerprints of virgin and used lubricating oils for identification of contamination or adulteration sources. Fuel 163, 271–281. https://doi.org/10.1016/J.FUEL.2015.09.070.

Yousaf, U., Khan, A.H.A., Farooqi, A., Muhammad, Y.S., Barros, R., Tamayo-Ramos, J.A., Iqbal, M. Yousaf, S., 2022. Interactive effect of biochar and compost with Poaceae and Fabaceae plants on remediation of total petroleum hydrocarbons in crude oil

contaminated soil. Chemosphere 286, 131782. https://doi.org/10.1016/j.chemosphere.2021.131782.